SAR Image Analysis, Modeling, & Techniques V

Vol. 4883

PROCEEDINGS OF SPIE
SPIE—The International Society for Optical Engineering

SAR Image Analysis, Modeling, and Techniques V

Francesco Posa
Chair/Editor

23–24 September 2002
Agia Pelagia, Crete, Greece

Sponsored and Published by
SPIE—The International Society for Optical Engineering

Cooperating Organizations
ISPRS—International Society for Photogrammetry and Remote Sensing
NASA—National Aeronautical Space Administration (USA)
European Optical Society
Hellenic Society for Photogrammetry and Remote Sensing (Greece)

Volume 4883

The papers published in this volume compose the proceedings of the technical conference cited on the cover and title page. Papers were selected by the conference program committee to be presented in oral or poster format, and were subject to review by the editors and program committee. They are published herein as submitted, in the interest of timely dissemination.

Please use the following format to cite material from this book:

Author(s), "Title of Paper," in Proceedings of SPIE Vol. 4883 *SAR Image Analysis, Modeling, and Techniques V*, edited by Francesco Posa, (SPIE, Bellingham, WA, 2002) page numbers.

ISSN 0277-786X
ISBN 0-8194-4665-3

Published by
SPIE—The International Society for Optical Engineering
P.O. Box 10, Bellingham, Washington 98227-0010 USA
Telephone 1 360/676-3290 (Pacific Time) · Fax 1 360/647-1445

Printed in the United States of America.

Conference Committee

Conference Chair

Francesco Posa, Politecnico di Bari (Italy)

Session Chairs

1 SAR Data Processing
Francesco Posa, Politecnico di Bari (Italy)

2 SAR Data Analysis
Francesco Posa, Politecnico di Bari (Italy)

3 SAR Images Classification
Giacomo De Carolis, IRA-CNR (Italy)

4 SAR Features Extraction
Giacomo De Carolis, IRA-CNR (Italy)

The Advanced Spaceborne Thermal Emission and Reflection Radiometer (ASTER)

Thomas Schmugge[a], Michael Abrams[b], Anne Kahle[b],Yasushi Yamaguchi[c], and Hiroyuki Fujisada[d]
[a]USDA Hydrology and Remote Sensing Lab, Beltsville, MD 20705, USA
[b]Jet Propulsion Laboratory 183-501, 4800 Oak Grove Dr., Pasadena, CA 91109
[c]Nagoya University, Nagoya, Japan
[d]Sensor Information Laboratory Corp., Tsukuba, Japan

Tel:301-504-8554, FAX:301-504-8931, email: schmugge@hydrolab.arsusda.gov

ABSTRACT

The Advanced Spaceborne Thermal Emission and Reflection Radiometer (ASTER) launched on NASA's Terra satellite in December 1999 provides anew tool for Earth observations. ASTER provides high-resolution, 15m(VNIR), 30m (SWIR) and 90m (TIR) coverage for limited areas with unique multispectal SWIR and TIR coverage and 15 m stereo coverage for DEM generation. These data have been used extensively for volcano and glacier monitoring. ASTER observations of over 1000 volcanoes around the world represent a significant increase in our ability to monitor volcanic activity and to map the products of eruptions. The SWIR channels have been used for mapping hot areas with temperatures up to 350 C and the multispectral TIR data have been used to map ash and SO_2 plumes. ASTER data are being used in the Global Land Ice Measurements from Space (GLIMS) project to map and catalog the approximately 80,000 glaciers. The objective is to acquire multiple observations to detect changes in ice margins and surface feature velocities. ASTER data acquired over the Jornada Experimental range in New Mexico have been used to extract spectral emissivities in the 8 to 12 micrometer range. These TIR data were also used in models to estimate the surface energy fluxes. Similar analysis of data acquired over the El Reno Oklahoma test site has shown that our satellite estimates of the surface fluxes agree reasonably well with ground measurements.

Keywords: Thermal infrared, remote sensing, ASTER, Terra

1. INTRODUCTION

Satellite sensors provide the only method to collect global data on a regular basis. NASA's Earth Science Enterprise (ESE) is working with international partners to design, build and launch advanced instruments to observe phenomena related to global change. ESE is comprised of four parts: 1) a series of satellites called the Earth Observing System (EOS), two of which, Terra (12/99) and Aqua (5/02), have been launched; 2) a series of smaller satellites; 3) a scientific research program; and 4) an EOS Data and Information System (EOSDIS) that provides a mechanism for storing and processing the data, and distributing them to the scientific community.

Terra was the first of a series of multi-instrument spacecraft forming NASA's Earth Observing System (EOS). EOS consists of a science component and a data system supporting a coordinated series of polar-orbiting and low inclination satellites for long-term global observations of the land surface, biosphere, solid Earth, atmosphere, and oceans. By enabling improved understanding of the Earth as an integrated system, the EOS program has benefits for us all. In addition to ASTER, the other instruments on Terra are the Moderate-Resolution Imaging Spectroradiometer (MODIS), Multi-angle Imaging Spectro-Radiometer (MISR), Clouds and the Earth's Radiant Energy System (CERES), and Measurements of Pollution in the Troposphere (MOPITT). As the only high spatial resolution instrument on Terra, ASTER is the "zoom lens" for the other instruments [1].

Data from ASTER are being used by scientists to study a wide range of problems dealing with the surface of the Earth, including vegetation change due to natural and human causes; monitoring and evaluating natural hazards such as volcanic eruptions; studying short term climate change and searching for reliable indicators of change, such as retreating or advancing

glaciers; monitoring sea ice extent and albedo; observing degradation of coral reefs as indicators of climate change or human effects; improved resource exploration; and for surface energy balance studies. An example of the latter application will be presented later in the paper.

To accomplish these tasks, ASTER provides observations in three spectral regions, as well as stereo observations, using three separate radiometers (Table 1). The Visible and Near-Infrared (VNIR) subsystem has three spectral bands covering 0.52-0.86 μm at 15 m resolution; the Short Wavelength Infrared (SWIR) subsystem has six spectral bands covering 1.60-2.45 μm at 30 m resolution; and the Thermal Infrared (TIR) subsystem has five spectral bands covering 8.125-11.65 μm at 90 m resolution. The VNIR system includes a separate, single spectral band radiometer inclined backward at an angle of 27.6° to provide an along-track stereo capability. The swath width is 60 km. Cross-track pointing allows viewing of any spot on Earth a minimum of once every 16 days. A wide dynamic range and selectable multiple gain settings help ensure useful signal-to-noise for a variety of investigations.

One of ASTER's primary goals is to obtain a cloud-free map of the land surface by the end of the six year mission. In addition, specific targets are observed in response to the science objectives of EOS investigators. The stereo capability is used to generate high-resolution digital elevation maps. Observations also include sites involving simultaneous ground measurements; targets of opportunity such as active volcanoes and major weather events; and high resolution observations of clouds.

Table 1. ASTER instrument specifications

Subsystem	Band	Bandwidth (μm)	Spatial Resolution
VNIR	1	0.52-0.60	15 m
8 Bit Quantization	2	0.63-0.69	
±24° Pointing	3N	0.76-0.86	
	3B	0.76-0.86	
SWIR	4	1.60-1.70	30 m
8 Bit Quantization	5	2.145-2.185	
±8.5° Pointing	6	2.185-2.225	
	7	2.235-2.285	
	8	2.295-2.365	
	9	2.360-2.430	
TIR	10	8.125-8.475	90 m
12 Bit Quantization	11	8.475-8.825	
±8.5° Pointing	12	8.925-9.275	
	13	10.25-10.95	
	14	10.95-11.65	

2. THE ASTER INSTRUMENT

ASTER is a cooperative effort between NASA and Japan's Ministry of Economy Trade and Industry (METI) formerly known as Ministry of International Trade and Industry (MITI), with the collaboration of scientific and industry organizations in both countries. The ASTER instrument consists of three separate instrument subsystems listed in Table 1. Each subsystem operates in a different spectral region, has its own telescope(s), and was built by a different Japanese company.

The Terra spacecraft is flying in a circular, near-polar orbit at an altitude of 705 km. The orbit is sun-synchronous with equatorial crossing at local time of 10:30 a.m., returning to the same orbit every 16 days. The orbit parameters are the same as those of Landsat 7, except for the local time.

2.1 The VNIR Instrument

The VNIR subsystem consists of two independent telescope assemblies to minimize image distortion in the backward and nadir looking telescopes. The detectors for each of the bands consist of 5000 element silicon charge coupled detectors (CCD's). Only 4000 of these detectors are used at any one time. A time lag occurs between the acquisition of the backward image and the nadir image. During this time earth rotation displaces the image center. The VNIR subsystem automatically extracts the correct 4000 pixels based on orbit position information supplied by the Terra platform.

The VNIR optical system is a reflecting-efracting improved Schmidt design. The backward looking telescope focal plane contains only a single detector array and uses an interference filter for wavelength discrimination. The focal plane of the nadir telescope contains 3 line arrays and uses a dichroic prism and interference filters for spectral separation allowing all three bands to view the same area simultaneously. The telescope and detectors are maintained at 296 ± 3K using thermal control and cooling from a platform provided cold plate. On-board calibration of the two VNIR telescopes is accomplished with either of two independent calibration devices for each telescope. The radiation source is a halogen lamp. A diverging beam from the lamp filament is input to the first optical element (Schmidt corrector) of the telescope subsystem filling part of the aperture. The detector elements are uniformly irradiated by this beam. In each calibration device, two silicon photo-diodes are used to monitor the radiance of the lamp. One photodiode monitors the filament directly and the second monitors the calibration beam just in front of the first optical element of the telescope. The temperature of the lamp base and the photo-diodes is also monitored. Provision for electrical calibration of the electronic components is also provided.

The system signal-to-noise is controlled by specifying the NE$\Delta\rho$ to be < 0.5% referenced to a diffuse target with a 70% albedo at the equator during equinox. The absolute radiometric accuracy is ± 4% or better. The VNIR subsystem produces by far the highest data rate of the three ASTER imaging subsystems. With all four bands operating (3 nadir and 1 backward) the data rate including image data, supplemental information and subsystem engineering data is 62 Mbps.

2.2 The SWIR Instrument

The SWIR subsystem uses a single aspheric refracting telescope . The detector in each of the six bands is a Platinum Silicide-Silicon (PtSi-Si) Schottky barrier linear array cooled to 80K. Cooling is provided by a split Stirling cycle cryocooler with opposed compressors and an active balancer to compensate for the expander displacer. The on-orbit design life of this cooler is to be 50,000 hours. Although ASTER operates with a low duty cycle (8% average data collection time) the cryocooler operates continuously because the cool-own and stabilization time is long. No cyrocooler has yet demonstrated this length of performance, and the development of this long-life cooler was one of several major technical challenges faced by the ASTER team.

The cryocooler is a major source of heat. Because the cooler is attached to the SWIR telescope, which must be free to move to provide cross-track pointing, this heat cannot be removed using a platform provided cold plate. This heat is transferred to a local radiator attached to the cooler compressor and radiated to space.

Six optical bandpass filters are used to provide the spectral separation. No prisms or dichroic elements are used for this purpose. A calibration device similar to that used for the VNIR subsystem is used for inflight calibration. The exception is that the SWIR subsystem has only one such device. The NE$\Delta\rho$ varies from 0.5 to 1.3% across the bands from short to long wavelength. The absolute radiometric accuracy is +4% or better. The combined data rate for all six SWIR bands, including supplementary telemetry and engineering telemetry, is 23 Mbps.

2.3 The TIR Instrument

The TIR subsystem uses a Newtonian catadioptric system with an aspheric primary mirror and lenses for aberration correction. Unlike the VNIR and SWIR telescopes, the telescope of the TIR subsystem is fixed with pointing and scanning done by a mirror. Each band uses 10 Mercury-Cadmium-Telluride (HgCdTe) detectors in a staggered array with optical band-pass filters over each detector element. Each detector has its own pre-and post-amplifier for a total of 50. As with the SWIR subsystem, the TIR subsystem uses a mechanical split Stirling cycle cooler for maintaining the detectors at 80K. In this case, since the cooler is fixed, the waste heat it generates is removed using a platform supplied cold plate.

The scanning mirror functions both for scanning and pointing. In the scanning mode the mirror oscillates at about 7 Hz. For calibration, the scanning mirror rotates 180 degrees from the nadir position to view an internal black body which can be heated or cooled. The scanning/pointing mirror design precludes a view of cold space, so at any one time only a one point temperature calibration can be effected. The system does contain a temperature controlled and monitored chopper to remove low frequency drift. In flight, a single point calibration is done frequently (e.g., every observation) if necessary. On a less frequent interval, the black body is cooled or heated (to a maximum temperature of 340K) to provide a multipoint thermal calibration. Facility for electrical calibration of the post-amplifiers is also provided.

For the TIR subsystem, the signal-to-noise can be expressed in terms of an NEΔT. The requirement is that the NE ΔT be less than 0.3K for all bands with a design goal of less than 0.2K. The signal reference for NEΔT is a blackbody emitter at 300K. The accuracy requirements on the TIR subsystem are given for each of several brightness temperature ranges as follows: 200 - 240K, 3K; 240 - 270K, 2K; 270 - 340K, 1K; and 340 - 370K, 2K. The total data rate for the TIR subsystem, including supplementary telemetry and engineering telemetry, is 4.2 Mbps. Because the TIR subsystem can return useful data both day and night, the duty cycle for this subsystem has been set at 16%. The cryocooler, like that of the SWIR subsystem, operates with a 100% duty cycle.

3. DATA PRODUCTS

The commitment to make Earth science data easily available to a wide community of users is implemented by the EOS Data and Information System (EOSDIS). EOSDIS is a comprehensive data and information system (Price et al., 1994) providing a range of services: user support; data archive management and distribution; information management; product generation; spacecraft command and control; and data capture and telemetry. Data products that are generated routinely for spatially and/or temporally extensive subsets of the data are called standard data products. For ASTER (and all other EOS instruments) the products are provided in Hierarchical Data Format (HDF) , and are defined by Level [2]:

Level 0: reconstructed, unprocessed instrument data at full resolution .

Level 1A: Reconstructed, unprocessed instrument data at full resolution, time-referenced, and annotated with ancillary information, including radiometric and geometric calibration coefficients and georeferencing parameters, computed and appended but not applied to the Level 0 data.

Level 1B: Level 1A data to which geometric and radiometric coefficients have been applied. The data from the 3 subsystems are co-registered.

Level 2: Derived geophysical variables at the same resolution and location as the Level 1 source data.

The ASTER instrument has two types of Level 1 data: Level 1A (L1A) and Level 1B (L1B). L1A data are formally defined as reconstructed, unprocessed instrument data at full resolution. The ASTER L1A data consist of the image data, the radiometric coefficients, the geometric coefficients and other auxiliary data without applying the coefficients to the image data, thus maintaining original data values. The L1B data are generated by applying these coefficients for radiometric calibration and geometric resampling.

All acquired image data are processed to L1A. Because of spacecraft on-board storage limitations, ASTER can acquire about 650 L1A scenes per day. A maximum of 310 scenes per day are processed to L1B based on cloud coverage.
The 1A and 1B data are archived at the EDC DAAC for distribution and processing to higher level data products.

3.1. Level-1 Products

The Level-1A data product consists of the image data, the radiometric coefficients, the geometric coefficients, and the auxiliary data [3]. The data are produced from raw Level-0 data. Data are separated by telescope (VNIR, SWIR, and TIR), and put into Band Sequential (BSQ) format. The radiometric coefficients are determined from pre-launch engineering measurements, and post-launch engineering and vicarious calibration determinations. The coefficients can be used to convert digital numbers in the Level-0 data to calibrated radiance at the sensor. In the TIR, on-board blackbody observations are used to calibrate the TIR signals. A wide range of geometric correction parameters are determined and stored as geometric coefficients. These include spacecraft attitude vectors, inter-telescope registration, intra-telescope band-to-band registration, etc. All of these factors are included in the Level-1A product, but they are not applied to the data. The data are reported in units of digital counts or digital numbers (DN). The VNIR and SWIR data are 8-bit and have a variable gain setting. The TIR data are 12-bit with a single gain . This form of data may be required by users who do not want their data resampled in any way, and need to analyze ASTER data in as raw a state as possible.

The Level-1B data are generated from the Level-1A data by applying the radiometric coefficients to calibrate the data to radiance-at-the-sensor; and by applying the geometric coefficients to produce the map projection requested by the user. These data are reported in units of radiance (watts per meter squared per steradian per micron). The user can also select the resampling method used for both of these transformations. This format is the one most users will probably order who want "raw" ASTER data, rather than derived higher level data products.

3.2. Level 2 Products

3.2.1 Decorrelation Stretch

The decorrelation stretch products are enhanced color composites of 3 bands from each of the telescopes. The processing algorithm is based on a forward and reverse principal components transformation, whose outputs are the original 3 bands with increased color saturation [4]. For the VNIR data, bands 3, 2 and 1 are displayed in red (R), green (G) and blue (B), respectively; for the SWIR, bands 8, 6 and 4 are displayed in RGB; for the TIR, bands 14, 12, and 10 are displayed in RGB.

3.2.2 Brightness Temperature at Sensor

The algorithm that computes brightness temperature uses a pre-computed table of values that represent observed radiance as a function of brightness temperature for a given sensor. The generation and inversion of this table are computationally expensive, but the results are constant for a given wavelength calibration of the sensors, and therefore, presumably, for the life of the mission. The table needs to be generated and inverted only once, prior to launch. Then, to generate the brightness temperature product for a given scene, one need only use the radiance value of each input pixel as the index to point to the desired brightness temperature in the stored table, and place the table values in the output dataset.

The input dataset for this product is the radiance observed at the sensor, in units of Watts per square meter per steradian per micrometer. The output product is reported in units of degrees centigrade, scaled by a factor of 100. For example, an output value of 2735 implies a brightness temperature of 27.35 degrees. Since the brightness temperature values are stored as 16 bit signed integers, the precision of the brightness temperature values is 0.01 degrees centigrade. When a brightness temperature product needs to be generated, the task is simply a matter of table lookup.

3.2.3 Surface radiance and reflectance-VNIR and SWIR

The algorithm used to calculate surface radiance and reflectance in the VNIR and SWIR wavelength regions (bands 1-9) relies on deriving a relationship between the surface radiance/reflectance and the top-of-the-atmosphere radiance from information regarding the scattering and absorbing characteristics of the atmosphere. This relationship is used to convert radiances measured by ASTER to surface radiance and reflectance.

Table 2. ASTER higher level data products							
Product ID	Level	Parameter Name	Production Mode	Units	Absolute Accuracy	Relative Accuracy	Spatial Resolution
AST06	2	D - Stretch	Routine	NA	NA	NA	15, 30, 90
AST04	2	T_B at Sensor	On-Demand	°C	1 -2 °C	0.3 °C	90
AST07	2	Surface Reflectance - VNIR, SWIR	On-Demand	none	4%	1%	15, 30
AST09	2	Surface Radiance VNIR, SWIR		W/ (m^2·ster·μm)	2%	1%	15, 30
AST09	2	Surface Radiance TIR		W/ (m^2·ster·μm			90
AST05	2	Surface Emissivity		none	0.05 - 0.1	0.005	90
AST08	2	Surface Kinetic Temperature		°K	1 - 4 K	0.3K	90
AST14	4	Digital Elevation Model (DEM)		m	≥ 7m	≥10m	30

The absorbing and scattering characteristics of the atmosphere are obtained from outside sources. The anticipated sources of this information are the results from MISR and MODIS sensors on Terra; we also anticipate using global assimilation model results. Difficulties arise when these sources of information are not available. For these situations, climatological data are used when no atmospheric information are provided.

The radiance product is reported in units of radiance (watts per meter squared per steradian per micron); the reflectance product is reported as a number between 0 and 1..

3.2.4 Surface radiance -TIR

The objectives of the ASTER investigation in the thermal infrared include, among other things, providing estimates of the radiance leaving the land surface . The radiance which is measured by the ASTER instrument includes emission, absorption and scattering by the constituents of the Earth's atmosphere. The purpose of the atmospheric correction method is to remove these effects providing estimates of the radiation emitted and reflected at the surface. Atmospheric corrections are necessary to isolate those features of the observation which are intrinsic to the surface, from those caused by the atmosphere. Only after accurate atmospheric correction can one proceed to study seasonal and annual surface changes and to attempt the extraction of surface kinetic temperatures and emissivities.

The approach used for atmospheric correction in the thermal infrared involves two fundamental elements: 1) the use of a radiation transfer model capable of estimating the magnitude of atmospheric emission, absorption and scattering and 2) the acquisition of all the necessary atmospheric parameters (e.g. temperature, water vapor, ozone, aerosol profiles) at the time and location of the measurement to be corrected.

The model used is MODTRAN [5]. The second element of the atmospheric correction approach involves identifying sources for all the necessary input atmospheric parameters that are either as accurate as necessary to meet the overall accuracy goal or are the best available. Most of these parameters are obtained from other sensors on the Terra platform instruments, or from assimilation models. The radiance product is reported in units of radiance (watts per meter squared per steradian per micron).

3.2.5 Temperature-emissivity separation

Accurate determination of surface kinetic temperature, as opposed to brightness temperature, requires knowledge of spectral emissivity. Temperature-emissivity separation (TES) algorithms are always approximations: separation is difficult because there are five measurements but six unknowns (5 emissivities and the temperature). Various approaches have been used to constrain the extra degree of freedom. TES operates on ASTER "land-leaving TIR radiance" data which have already been corrected for atmospheric transmission and upwelling radiance. ASTER's TES algorithm [6] hybridizes three established algorithms, first estimating the temperature by the normalized emissivity method, and then using it to calculate unbiased emissivity band ratios. An empirical relationship [7] predicts the minimum emissivity from the spectral contrast (min-max difference or MMD) of the ratioed values [8], permitting recovery of the emissivity spectrum. TES uses an iterative approach to remove reflected sky irradiance. Based on numerical simulation, TES can recover temperatures within about ±1.5K, and emissivities within about ±0.015. Limitations arise from the empirical relationship between emissivity values and spectral contrast, compensation for reflected sky irradiance, and ASTER's precision, calibration, and atmospheric correction. Output products are:

Surface Kinetic Temperature is a single image plane consisting of short-integer (16-bit) pixels specifying the temperature in quanta of 0.1K. Output is T multiplied by 10.

Surface Emissivity is coded in five image planes consisting of 16-bit pixels specifying the emissivity in quanta of 0.001. Output is multiplied by 1000. The possible emissivity range of 0-1 is thus encoded as 0 – 1000.

3.2.6 Digital Elevation Model

The ASTER stereoscopic subsystem consists of nadir and rear-viewing telescopes operating in the visible-near infrared wavelengths (band 3). This subsystem, configured to provide a base-to-height ratio of 0.6, acquires along-track, digital stereo data at 15 m resolution over a 60 km ground swath . Digital Elevation Models (DEMs) are produced from the ASTER Level 1A input data [9].

A digital stereo correlation approach is used to calculate parallax differences and derive DEMs from ASTER stereo pairs. ASTER standard product DEM production uses commercial off-the-shelf photogrammetric software and hardware that implement the procedure. The DEM standard data product is produced at a rate of one scene per day.

The process for generating DEMs starts with the construction of a stereo pair by registering two images of the same ground area recorded from different positions in space. In the stereo pair, any positional differences parallel to the direction of satellite travel (parallax differences) are attributed to displacements caused by relief. Relative ground elevations are determined by measuring parallax differences in the registered images. True or absolute elevations (Z-coordinates) are determined in a subsequent step.

DEM accuracies depend on the presence or absence of Ground Control Points (GCPs), provided by a data requester. In the absence of GCPs, the relative DEM has an accuracy of 15-30 m. The availability of accurate GCPs allows production of absolute DEMs with accuracies depending on the number and quality of control points. ASTER DEMs can be combined with image data to produce 3-D perspective views or visualizations

3.3 Obtaining ASTER Data

ASTER data are available through EOSDIS by using an on-line web-based search and order tool. Any data that have already been acquired are available to all by submitting a Data Request. A data processing request is submitted through the search tool at the Land Processes DAAC. (http://edcimswww.cr.usgs.gov/pub/imswelcome/). This tool allows the user to search the database of ASTER scenes to determine if data have been acquired over the user's study area. If data have been acquired the tool allows the user to order the data. However, ASTER is also an on-demand instrument. This means data will only be acquired over a location if a Data Acquisition Request (DAR) has been submitted. Registered users can submit a data

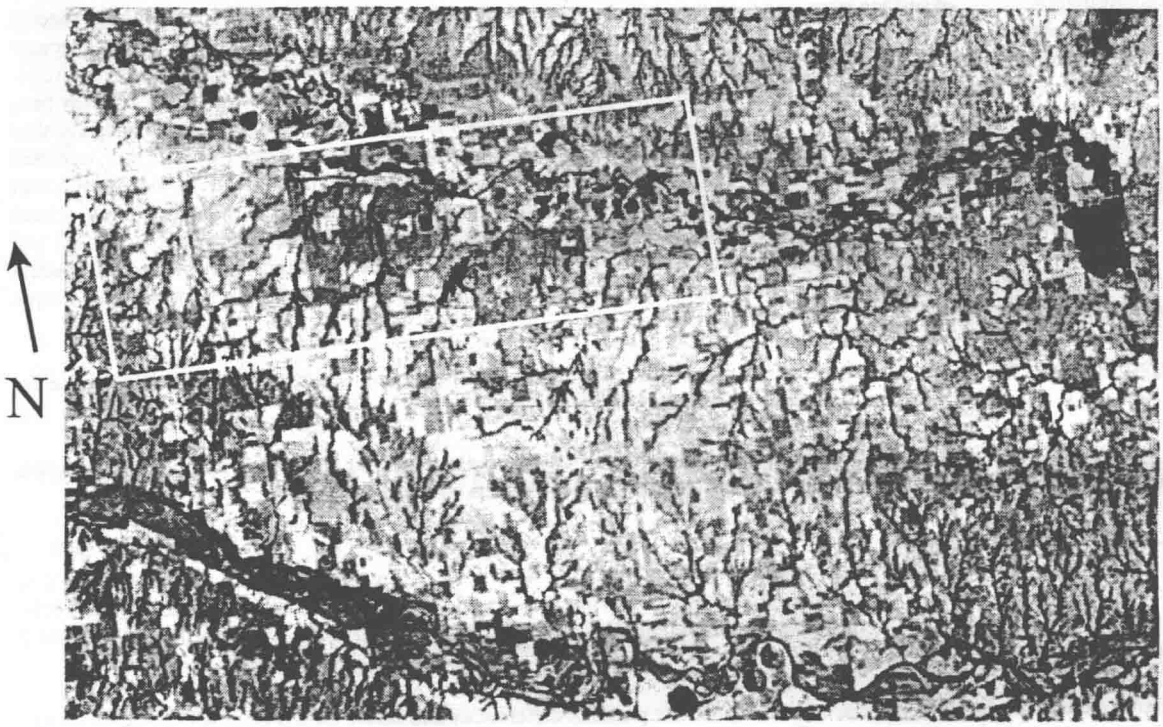

Figure 1. ASTER TIR imagery for a region in central Oklahoma, just west of Oklahoma City. The data were taken on September 4, 2000 at 17:34 GMT and are for band 13 of ASTER, λ = 10.7 μm. The temperatures range from 36 C (black) to 57 C (white).

acquisition request via the Data Acquisition Request Tool . In order to use this tool users must first register and receive approval from a committee consisting of NASA Headquarters officials, ASTER Science Team members, and other scientists. For more information please visit the ASTER web site at "http://asterweb.jpl.nasa.gov" where the ASTER User Handbook can be obtained [10].

4. RESULTS

4.1 Observations of Surface Energy Fluxes

The monitoring of the land surface fluxes at large or regional scales is recognized as important for applications as the modeling of atmospheric behavior, the evaluation of crop health and the monitoring of water resources. Typical approaches towards estimating evapotranspiration are developed around a surface energy balance model with four components: net radiation (R_n), soil heat flux (G), sensible heat flux (H), and latent heat flux (LE). In these models, incoming solar energy energy is balanced by outgoing energy to the soil and the surface boundary layer. The desired evapotranspiration is represented by the LE component. Spatially distributed surface energy flux estimates are difficult to make, especially over heterogeneous terrain. One of the most reliable techniques available for measuring surface fluxes is with eddy-covariance instruments, but experience has shown that there may be large variabilities in measurements at closely located sites. Remote sensing techniques excel at characterizing spatial relationships of surface features, but cannot make critical observations of near surface temperatures, winds and humidity. The most promising approach to measuring evapotranspiration, therefore,

lies in using a model that combines ground-based measurements with reliably calibrated remote sensing data. In the past, this approach has been hindered by inadequate spatial resolutions and by unreliable surface temperature estimates. ASTER is an excellent source of remotely sensed data which can be applied to this problem.

An example of ASTER TIR data is presented in figure 1 for central Oklahoma in the United States. [11] The large variations in surface brightness or radiant temperatures, T_R, which are observed arise from differences in the surface energy balance for the land surfaces. Recall that T_R is a measure of the emitted radiation from the surface is directly related to the temperature of the surface and its emissivity. The temperature contrasts seen between fields with different vegetation conditions imply a different partition of the incoming solar energy into latent and sensible heat components. Cooler temperatures usually indicate that there is sufficient moisture available so that most of the incoming energy goes into latent heat or evaporation, in this case they are usually pasture grass or vegetated stream channels. While hotter temperatures indicate that most of the incoming energy goes into the sensible or convective heating of the atmosphere, here they are generally bare soils which were planted to winter wheat later in the fall. However there is another aspect of the problem of determining the surface fluxes which arises due to the differences in the heat transfer coefficients arising from the various types of vegetation and their heights. Thus the wooded areas along the drainages can be just as cool as a well-watered field but transpiring much less because of their greater heat transfer capability.

ASTER observations in the VNIR and TIR are used to estimate the surface temperature and the normalized difference vegetation index (NDVI) for use in a relatively simple, physically-based surface energy flux model along with commonly available surface meteorological observations [11], [12]. Resulting estimates of evapotranspiration appear to be reasonable and form a basis for further development of remote sensing based flux models. The data were obtained over the USDA/ARS Grazinglands Research Laboratory near the town of El Reno in central Oklahoma. The fields typically span hundreds of meters and include grasslands, pasture and winter wheat., Within the core grasslands, there is a field site containing Bowen Ratio instruments which collect energy flux and local meteorological measurements. The flux data from this station were compared with the ASTER based model estimates.

4.2 Two Source Model

The model used, a two source energy balance (TSEB) model, considers the contributions from the soil and canopy separately and which requires only a few additional parameters for implementation [13],[14]. The essence of TSEB is the partitioning of the turbulent surface energy flux components - H the sensible heat flux and LE the latent heat or moisture flux into the atmosphere - into two sources: vegetation canopy and soil, for each surface element. The partitioning is accomplished by estimating fractional vegetative cover from the normalized difference vegetation index (NDVI), proportioning the observed radiometric. Although the input requirements are modest, TSEB output is strongly controlled by physically meaningful observations, and less so by strictly empirical relationships.

The surface energy balance is evaluated for each elemental area (defined by the pixel size of remotely sensed data), i, using the dual-source model. In this model the soil surface and vegetative canopy fluxes are considered in parallel with their own resistance to heat transfer.

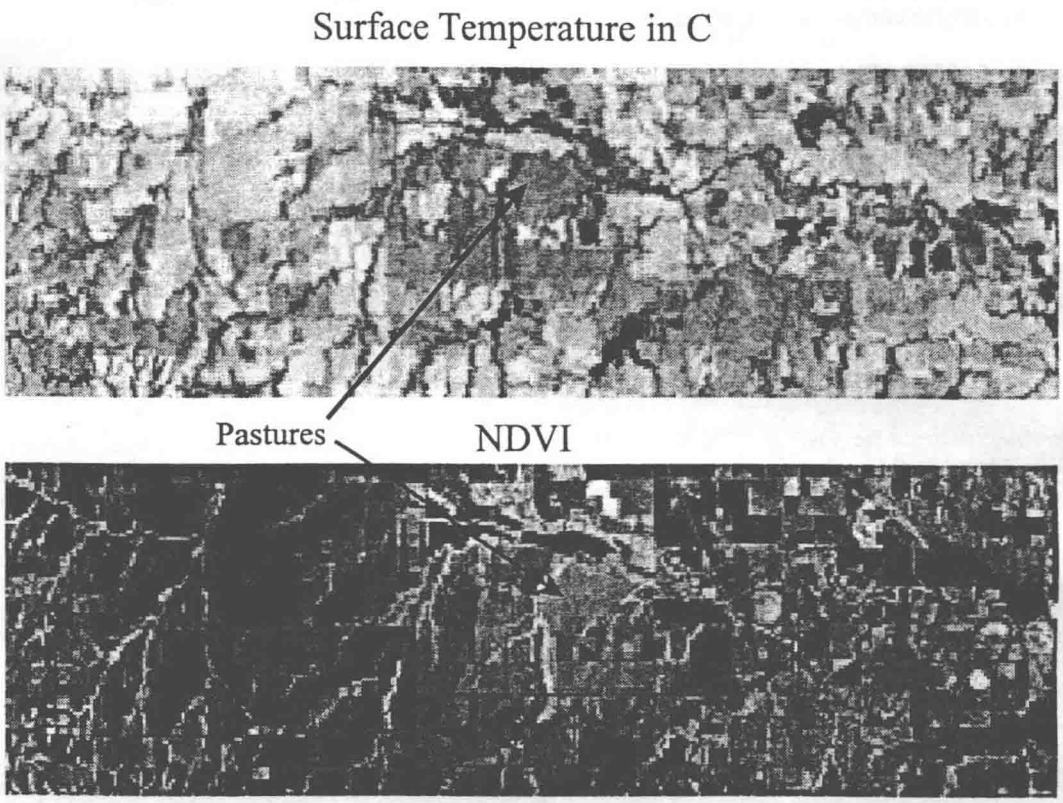

Figure 2. Surface temperatures and ndvi values for the portion of figure 1 outlined by the white box. The area is approximately 30 by 8 km. The temperatures range from 36 to 57 C and the ndvi values range from -0.1 to 0.5.

4.2 Results

Figure 2 presents the temperature and NDVI values that were used is the analysis for the September 4 scene. The temperatures are the output from the TES procedure and are representative of the physical or kinetic temperature of the surface. The grass pastures are indicated by the arrows. They are seen to be in the low to mid range of temperature and toward the high end of NDVI values. The regions with high temperatures and low NDVI values toward the west of the images are bare fields which are or will be planted to winter wheat. Similar images were obtained on September 27 and November 21 and analyzed. The results show reasonably close agreement for early September, when senescense was just beginning. Late September results were improved when assumptions about vegetative cover were derived from SGP97 observations [15], rather than from ASTER observations directly. The results show that ASTER observations of surface temperature and NDVI are as expected and that reliable surface flux estimates are feasible. The discrepancy for the November scene highlights a difficulty encountered by all remote sensing energy flux models, namely how to quantify vegetative cover during senescence. We also note that the model ground heat flux values are high and may have to be adjusted in the future.

Table 3. Flux comparisons in W/m^2

Date	Sensible Heat H		Latent Heat LE		Soil Heat Flux G		Net Radiation R_n	
	EBBR	TSEB	EBBR	TSEB	EBBR	TSEB	EBBR	TSEB
Sept. 04, 2000	249	147	236	233	26	63	510	444
Sept. 27, 2000	374	333	103	137	22	44	499	514
Nov. 21, 2000	235	100	61	135	9	52	304	286

Integration of the instantaneous LE values from 4 September observations resulted in a daily evapotranspiration image shown in Figure 3. The integration is based on the measured diurnal variation of the incoming solar radiation. This approach is similar to the evaporative fraction approach developed by Shuttleworth et al. [16]. The patterns are consistent with known land uses: low evapotranspiration over dry, unvegetated soils, and higher evapotranspiration over well vegetated fields. Water bodies and riparian zones also show relatively high evapotranspiration.

Additional ASTER scenes over El Reno from June and July 2001 will be used to help determine if these discrepancies between the ground observations and the model estimates persist under other conditions, and how they might be ameliorated.

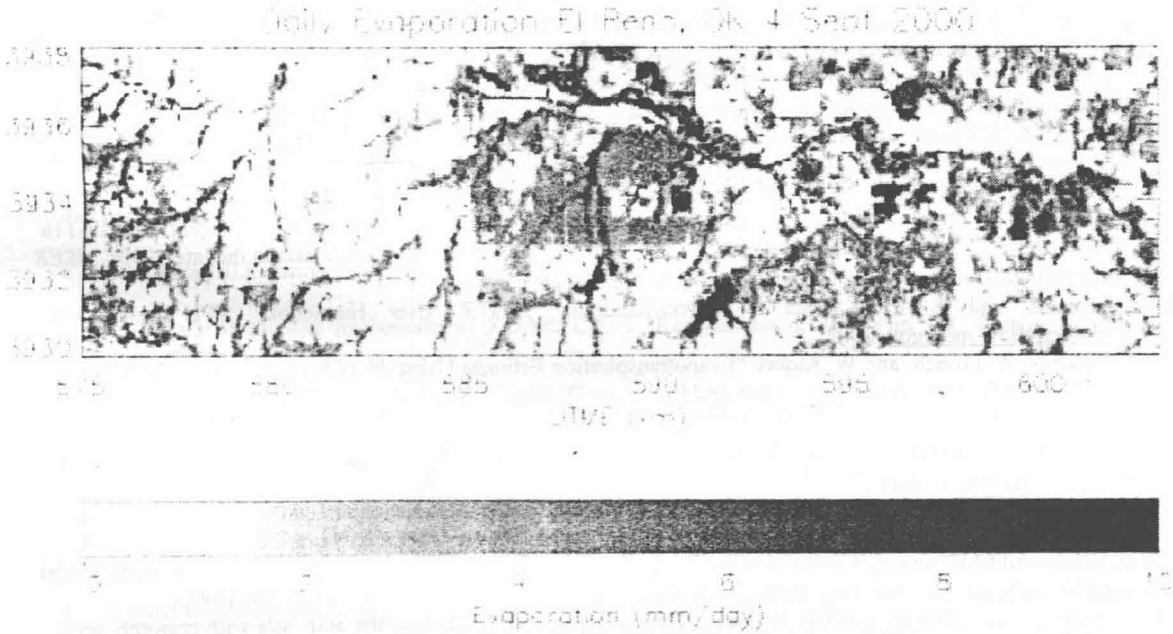

Figure 3.Estimated daily evapotranspiration over the El Reno, Oklahoma study area using ASTER observation at about 11:30am. A drought occurred during the summer of 2000 , and by September many of the fields were either plowed or contained senescent vegetation. In this image, 0-1 corresponds to dry soils, 4 to grass lands, and 6-8 to lakes, ponds and riparian zones

5. CONCLUSIONS

The ASTER instrument is the logical follow-on to the Landsat Thematic Mapper instrument in regards to extending the capabilities of a global data acquisition, high spatial resolution imager. ASTER is the first satellite imager to obtain multispectral thermal infrared data and simultaneously acquired high resolution stereo data. Data are available to everyone through a web-based search and order system. In addition, approved investigators are able to command the instrument to acquire specific data for their individual investigations, tailoring the instrument configuration to their viewing needs. In this regard, ASTER is unique; and is providing the earth science community with an unparalleled set of data for scientific research.

ACKNOWLEDGMENTS

This work was supported by the ASTER project of NASA's EOS-Terra program.

REFERENCES

[1] Y. Yamaguchi, A. Kahle, H. Tsu, T. Kawakami, and M. Pniel, "Overview of Advanced Spaceborne Thermal Emission and Reflection Radiometer (ASTER)". *IEEE Transactions on Geoscience and Remote Sensing*, **36**, 1062-1071, 1998.

[2] M. Abrams, "The Advance Spaceborne Thermal Emission and Reflection Radiometer (ASTER): data products for the high spatial resolution imager on NASA's Terra platform," *Int. J. Remote Sensing*, **21**, pp. 847-859, 2000.

[3] H. Fujisada, "ASTER Level-1 data processing algorithm," *IEEE Transactions on Geoscience and Remote Sensing*, **36**, 1101-1112, 1998.

[4] A. Gillespie, A. Kahle, and R. Walker, "Color enhancement of highly correlated images. I. Decorrelation and HSI contrast stretches". *Remote Sensing of Environment*, **20**, 209-235, 1986..

[5] L. Abreu, F. Kneizys, G. Anderson, J. Chetwynd, A. Berk, L Bernstein, and D. Robertson, "MODTRAN". *Proceedings 1991 Battlefield Atmospherics Conference, El Paso TX*, 1991.

[6] A. Gillespie, T. Matsunaga, S. Rokugawa, and S. Hook, "A temperature and emissivity separation algorithm for ASTER images," *IEEE Transactions on Geoscience and Remote Sensing*, **36**, 1113-1126, 1998.

[7] T. Matsunaga, "A Temperature-Emissivity Separation Method Using an Empirical Relationship between the Mean, the Maximum, and the Minimum of the Thermal Infrared Emissivity Spectrum.," *Journal of Remote Sensing Society of Japan*, **14(2)**, 230-241, (in Japanese with English abstract) 1994.

[8] K. Watson, 1992. Spectral ratio method for measuring emissivity. *Remote Sensing of the Environment*, **42**, 113-116.

[9] R. Welch, T. Jordan, H. Lang, and H. Murakami, "ASTER as a source for topographic data in the late 1990s," *IEEE Transactions on Geoscience and Remote Sensing*, **36**, 1282-1289, 1998..

[10] M. Abrams and S. Hook, and B. Ramachandran, "ASTER User Handbook," JPL publication," http://asterweb.jpl.nasa.gov, 2002.

[11] T. Schmugge, A. French, and W. Kustas, "Evapotranspiration Estimate Using ASTER Thermal Infrared Imagery," *Remote Sensing for Agriculture, Ecosystems, and Hydrology III*, Manfred Owe, and Guido D'Urso, Editors, Proceedings of SPIE Vol. **4542** (2002) © 2002 SPIE · 0277-786X/02/$15.00.

[12] A.N. French, T.J. Schmugge, and W.P Kustas, "Estimating evapotranspiration over El Reno, Oklahoma with ASTER imagery," *Agronomie*, **22**, pp. 105–106, 2002.

[13] J.M Norman, W.P. Kustas, and K.S. Humes, "A two-source approach for estimating soil and vegetation energy fluxes from observations of directional radiometric surface temperature," *Agric. Forest Meteorol.*, **77**, pp. 263-293, 1995.

[14] W.P. Kustas and J.M Norman, "Evaluation of soil and vegetation heat flux predictions using a simple two source model with radiometric temperatures for partial canopy cover," *Agric. Forest Meteorol.*, **94**, pp.13-29, 1999.

[15] A.N. French, T.J. Schmugge, and W.P Kustas, "Estimating surface fluxes over the SGP site with remotely sensed data," *Physics and Chemistry of the Earth*, **25 (2)**:167-172, 2000.

[16] W.J. Shuttleworth, R.J. Gurney, A.Y. Hsu, and J.P. Ormsby, "FIFE, the variation on enery partition at surface flux sites". *Proc. IAHS Third Intl. Assembly*, IAHS Publ. No. 186, pp. 67-74, 1989.

Contents